Stability and Control of Maneuvering High-Performance Aircraft

Robert F. Stengel* and Paul W. Berry†
The Analytic Sciences Corporation, Reading, Mass.

Stability and control characteristics of a high-performance aircraft have been examined over a wide range of maneuvering flight conditions, in order to identify methods for the design of departure-preventing control systems. This has been accomplished using fully coupled linear dynamic models, which account for nonzero mean values of aerodynamic angles and angular rates. Stability augmentation systems derived from optimal control theory are shown to maintain stable well-damped aircraft dynamics over a wide range of maneuvering flight conditions. This design approach generates crossfeeds and control interconnects (as well as conventional feedback terms) for improved aircraft stability.

Introduction

As aircraft become capable of flying higher, faster, and with more maneuverability, prevention of inadvertent departure from controlled flight takes on added significance. To some extent, the airframe can be designed to provide inherent protection against loss of control; however, performance objectives often dominate the choice of aircraft configuration. It is likely, therefore, that the freedom to configure the aircraft for intrinsic departure prevention will be restricted, and that the flight control system will be called upon to provide additional protection.

Flight at high angle-of-attack α invariably complicates the control problem. Dynamic coupling between longitudinal and lateral-directional motions can become significant, and control surface effects can diminish or become adverse. Abrupt maneuvering, external disturbances, or pilot error can produce a "departure" (pitch, yaw, or roll divergence), which can lead to loss of control and to a fully developed spin. The combined effects of nonzero mean motions lead to significant coupling, which otherwise might be missed in a linear dynamic model. The complexity of the coupled dynamics and the possibility for misinterpreted control cues at high α indicate a need for departure-preventing control systems in highly maneuverable aircraft.

The purpose of the investigation reported here and in Ref. 1 is to identify general rules for the design of departure-preventing control systems. In achieving this objective, the analytic foundations for linear-time-invariant modeling of aircraft dynamics are extended to include extreme maneuvering conditions. By using tools of linear systems analysis, the stability and control characteristics of a high-performance aircraft are examined over a wide range of flight conditions. The study culminates in the development and evaluation of control laws for a departure-prevention stability augmentation system (DPSAS), using linear-optimal control theory. Results presented here strictly apply to a single "reference aircraft," and care should be exercised in extending these results to other configurations.

Dynamic Characteristics of a High-Performance Aircraft

The problems associated with extreme maneuvering have two common characteristics: loss of control and large angles and/or angular rates, i.e., angles and rates generally beyond the range of normal, 1-g flight operations. Extreme maneuvering difficulties fall in the following categories, which contain some overlap: decreased inherent stability, degraded handling qualities, longitudinal/lateral-directional coupling, stall, wing rock, departure, post-stall gyrations, incipient spin, and fully evolved spin.

Received June 30, 1976; presented as Paper 76-1973 at the AIAA Guidance and Control Conference, San Diego, Calif., Aug. 16-18, 1976 (in bound volume of Conference papers); revision received April 15, 1977.

Index categories: Handling Qualities, Stability, and Control; Guidance and Control; Flight Operations.

*Member of the Technical Staff. Associate Fellow AIAA.

†Member of the Technical Staff. Member AIAA.

Prior Studies of Aircraft at Extreme Flight Conditions

Three fundamentally different avenues have been followed in the investigation of maneuvering flight. The first approach is the study of rigid-body dynamics of the aircraft,[2-5] the second is the study of aerodynamics,[6,7] and the third is the study of control.[8,9] The first two areas have a cause-and-effect relationship – aerodynamic forces modify the momentum and energy of the airplane – and there is a "feedback," in the sense that the changing velocity and attitude of the vehicle contribute to changes in the aerodynamic forces. The third area considers methods of augmenting the natural aircraft stability, of limiting excursions from the normal flight regime, of providing adequate response, and of recovering from fully evolved spins. A further discussion of these areas and an extensive list of references are contained in Ref. 1; the remainder of this paper treats new topics in dynamics and control.

Comparison of Linear and Nonlinear Results

The use of linear models in highly dynamic situations has been restricted, in the past, by a lack of linear models which include complete dynamic coupling effects and by the lack of a general method of finding the proper nominal flight condition. In order to verify these models and to develop methods of using them, a brief comparison of linear and nonlinear results is presented. The nonlinear results are in the form of test trajectories generated by a nonlinear aircraft simulation using aerodynamic and mass data for the "reference aircraft," a composite of subscale wind-tunnel measurements for the F-5A and E configurations.

During the early part of the investigation, large differences between the linear and nonlinear results appeared along highly dynamic flight trajectories. These were traced to the use of an incorrect nominal state vector. From these observations, the concept of generalized trim was developed.[1] The generalized trim condition is one in which the derivatives of the velocity and angular rate states are as close to zero as possible. Those values of nominal body-axis velocities and angular rates that null the selected nominal state rates must be found by numerical search.

Figure 1 compares the nonlinear trajectory resulting from a large rudder input to a linear trajectory starting at the time of control application. The altitude is 6096 m (20,000 ft), and the

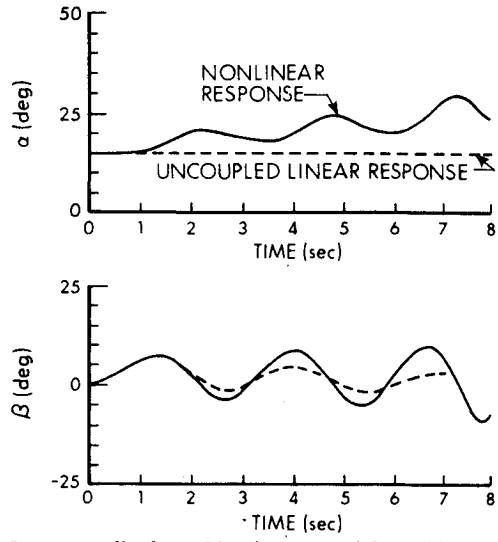

Fig. 1 Large amplitude rudder input; straight-and-level nominal trajectory for linearization.

air speed is 94 m/sec (307 ft/sec). The linearization assumes straight-and-level flight. The trajectory match is acceptable for only two seconds, and the angle-of-attack plot illustrates the cause of the deviation; the linear trajectory does not capture the change in angle of attack that the nonlinear trajectory contains. This change in angle of attack has a large effect on the subsequent dynamics, which the linear model fails to duplicate.

Applying the generalized trim procedure to the point 4 sec after control application produces the results shown in Fig. 2. The generalized trim procedure produces superior results. There are no initial slope errors evident, the match is excellent for 2 sec (it is reasonably close for much longer), and the frequency of the linearized motions is close to that of the nonlinear trajectory. The significance of this result is put in proper perspective when it is realized that the vehicle has performed a 270° roll between $t = 4$ and $t = 8$ sec.

Effects of Flight Condition on Aircraft Stability

The effects of angle-of-attack and sideslip angle variations and steady angular rates on aircraft stability are examined in this section using linearized dynamic models. The aircraft is trimmed initially for 1-g flight at an angle of attack of 15 deg, a true air speed of 94 m/sec, and an altitude of 6096 m.

Aerodynamic Angle Effects

The aerodynamic angles α_0 and β_0 specify the orientation of the vehicle relative to the velocity vector, and, to a large extent, they define the flowfield around the vehicle. Consequently, significant differences in the normal modes of motion occur as α_0 and β_0 are varied.

Figure 3 illustrates the boundaries between stability and instability which result from these variations. The phugoid mode is a slow longitudinal mode, and it is unstable at low α_0. The Dutch roll mode, a fast lateral-directional mode becomes unstable at high α_0. The dashed line indicates the transition of a slowly divergent phugoid oscillation into two real roots, one of which is highly unstable. Moderate values of nominal sideslip angle (2°-5°) stabilize the Dutch roll mode. This is because of longitudinal/lateral-directional coupling; up to about 5° of sideslip, Dutch roll damping increases as short period damping decreases.

The eigenvectors of the linearized model (not shown) provide information about the normal mode shapes which indicate the involvement of each state in each mode.[10] Longitudinal/lateral-directional coupling is quite prominent for asymmetric flight conditions.[1] Roll angle response is found in the phugoid mode, and pitch angle becomes a

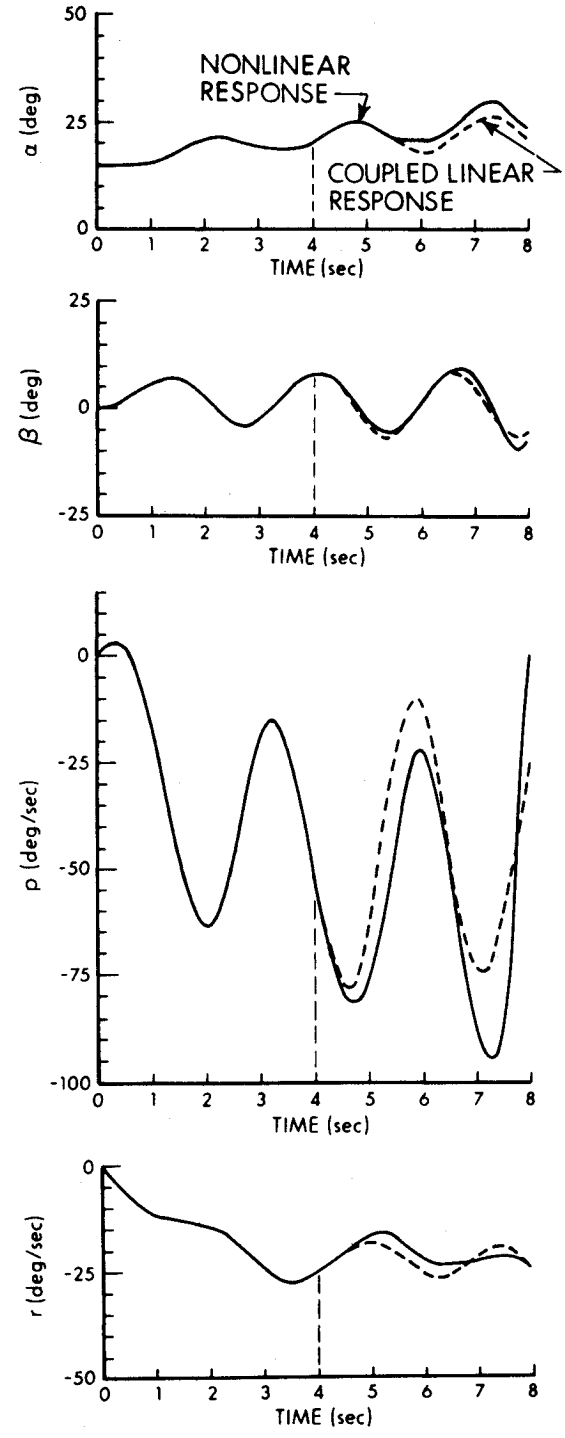

Fig. 2 Large amplitude rudder input; linearization with $\alpha_0 = 22.9°$, $\beta_0 = 1.6°$, $p_0 = -51.7$ deg/sec, $q_0 = 10.5$ deg/sec, $r_0 = -26.0$ deg/sec, $\delta_{r_0} = 30°$ (generalized trim point).

component of the spiral mode, so that both modes involve slow roll-pitch motion. Angle of attack appears in the Dutch roll eigenvector, and a roll-sideslip combination becomes important in the short period mode, so that both modes involve an angle of attack-sideslip oscillation.

Angular Rate Effects

Nonzero nominal angular rates have two effects on the linearized aircraft dynamics. The first, an aerodynamic effect, results in a change in the nominal forces and moments due to the steady angular rates. The second is dynamic, and it is due to the cross product of angular rate with velocity (in the force equations) and with angular momentum (in the moment

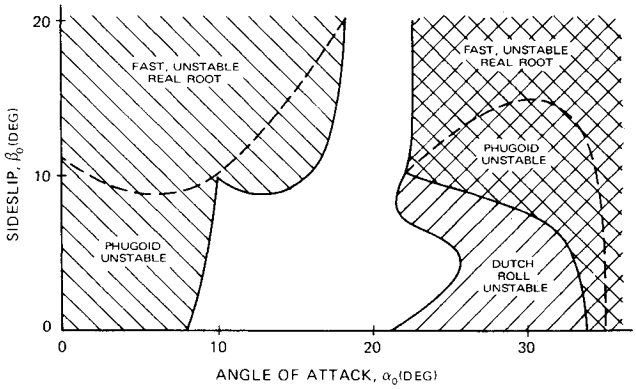

Fig. 3 Effects of aerodynamic angles on aircraft stability.

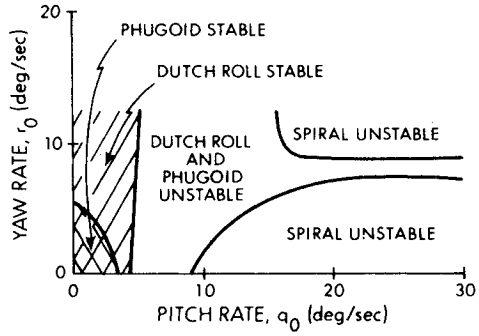

Fig. 4 Yaw-rate/pitch-rate effects on aircraft stability boundaries.

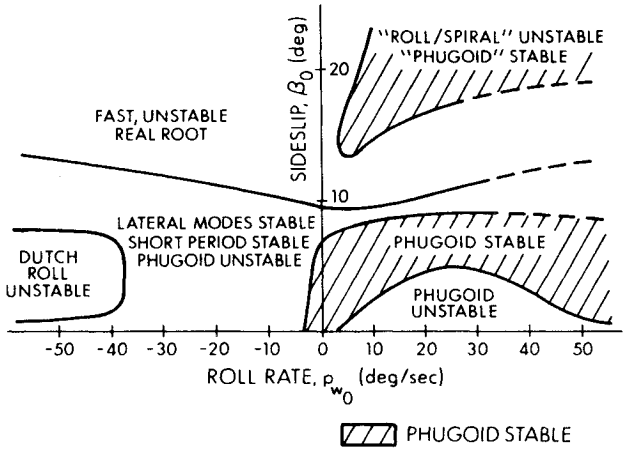

Fig. 5 Stability boundaries for sideslip/roll-rate variations.

equations). Mean pitch angular rate q_0 enters both the lateral and longitudinal equations, but does not affect longitudinal/lateral-directional coupling terms. Mean roll and yaw rates p_0 and r_0 enter as longitudinal/lateral-directional coupling terms. The steady roll-rate capability of most high-performance aircraft is much higher than pitch- or yaw-rate capability, so that roll-rate effects are especially important.

Stability boundaries as functions of pitch rate and yaw rate are illustrated in Fig. 4. The destabilizing influence of q_0 is the major effect, and it has an especially severe impact on the Dutch roll mode. Yaw rate has a mild stabilizing effect on the Dutch roll and spiral modes. This is partially because of longitudinal/lateral-directional coupling; short period and phugoid damping decrease as Dutch roll damping increases.

The stability boundaries for combined wind-axis roll rate p_{w_0} and sideslip are shown in Fig. 5. These boundaries indicate that the combination of p_{w_0} and small values of β_0 of opposite sign serves to destabilize the Dutch roll mode. Roll rate destabilizes the phugoid mode in general, but there is a combination of β_0 and p_{w_0} which maintains phugoid stability. High β_0 results in a fast divergence for all values of p_{w_0} tested.

Eigenvector variations due to steady rolling (not shown) indicate the extent of cross-axis coupling which occurs in this asymmetric flight condition.[1] Not only does roll rate enter the short period mode, but there is substantial interrelationship in the roll, spiral, and phugoid modes.

Open-Loop Control Effects

Aerodynamic angle variations can cause large changes in the system eigenvalues and can be expected to have significant effects on the numerators of control transfer functions as well. One of the major effects of angle-of-attack variations is the loss of aileron roll control at high α_0. As in many cases, this aircraft is rolled more effectively with the rudder at high angles of attack.

An examination of transfer function zeros indicates that nonminimum-phase zeros are quite prevalent, although often accompanied by right-half-plane poles, i.e., they often occur in unstable systems. When β_0 is not zero, there is mode coupling, and a control input excites all modes. Although no explicit effects of nominal angular rates on the control effectiveness are included in the specific aerodynamic data used here, angular rates also cause significant changes in the transfer functions.

Dynamic Variations during Extreme Maneuvering

Aircraft may be especially prone to departure from controlled flight during air combat maneuvering.[11] Even small errors can cause difficulty due to instability, unfamiliar coupled mode shapes, or changes in control effectiveness.

Many air combat maneuvers include periods of high angular rates and high-angle-of-attack flight, in order to produce a large normal force for climbing or turning. High normal acceleration may be accompanied by large q_0, and large p_0 may be generated to orient the lift force rapidly in a desired direction. High angles of attack and pitch rate destabilize the normal modes of motion and reduce the available control power, whereas high roll rate causes longitudinal/lateral-directional coupling and produces mode shapes that may be unfamiliar to the pilot.

As an example, a rolling reversal combines a rapid pullup with a rapid rolling maneuver, resulting in a "corkscrew-like" path through space. The combination of a high-acceleration pullup and rapid rolling produces unstable modes with considerable longitudinal/lateral-directional coupling. Maneuver altitude is 6096 m (20,000 ft); initial and final air speeds are 217 m/sec (715 ft/sec) and 152 m/sec (501 ft/sec), respectively. The eigenvalues shown in Table 1 illustrate the changes in aircraft stability as the rolling reversal progresses. Because of the high q_0 involved in this 22-sec maneuver, the Dutch roll mode is unstable throughout most of the maneuver.

The aircraft control effectiveness follows trends similar to the aircraft stability, i.e., the control effectiveness is degraded throughout the first half of the maneuver, but it improves during the second half. This difficulty is complicated by high angular rates, longitudinal/lateral-directional coupling, and extreme attitudes.

Classification of Departures

Unforced departures are due to instabilities in the basic aircraft. If the pilot does not move the controls, the aircraft states build up until the aircraft can no longer be controlled. In a forced departure, the basic aircraft may or may not be unstable, but the addition of a pilot loop closure creates an unstable vehicle-pilot system.

Unforced Departure Modes

Unforced departures occur when the pilot cannot or does not stabilize an unstable vehicle. The vehicle eigenvalues

Table 1 Rolling reversal eigenvalues

Working Point	Short Period	Dutch Roll	Roll	Spiral	Phugoid
High-g Pullup	-0.87 ±j4.1	0.19 ±j4.5	-0.91	0.14	-0.18, -0.06[a]
Roll	-0.69 ±j3.2	0.18 ±j3.6	-0.72	-0.17	0.01 ±j0.41
Roll	-0.40 ±j1.9	0.11 ±j2.1	-0.41	-0.22	0.12 ±j0.12
Roll and Pullup	-0.39 ±j2.3	0.13 ±j2.7	-0.71	-0.09	-0.15 ±j0.12
Pullup	-0.59 ±j1.8	-0.01 ±j3.8	-0.82	-0.08	-0.07 ±j0.10

[a] Real roots

directly indicate the open-loop system stability in this case, so that many of the stability boundaries that have been shown in this paper can be classed as unforced departure boundaries.

"Reference aircraft" aerodynamics have been modified to illustrate departure types in Figs. 6-8. A departure caused by directional instability is shown in Fig. 6. Although the linear model indicates that this motion is an oscillation, it is so unstable that only part of one cycle appears on the time history plot. The first few seconds of the motion exhibit a rapid roll-yaw angular motion. The pilot would sense a rapid rotational divergence about this axis and might refer to it as a rolling nose slice, or yaw departure.

Negative yaw damping destabilizes the Dutch roll mode. The time history of a departure due to dynamic Dutch roll instability is shown in Fig. 7, and the difference in shape from the departure due to static instability is apparent. The large amount of rolling motion in the Dutch roll mode indicates that this may be what pilots refer to as wing rock. A pilot sensing such as oscillation probably would unload the aircraft by reducing the angle of attack, removing the aircraft from the region of instability.

Forced Departure Modes

Control inputs from a pilot or control system can force an aircraft to depart from controlled flight in two ways. In the first case, adverse response to pilot inputs moves the nominal flight condition into an unstable region where an unforced departure can occur. The second possible cause of a forced departure is an improper loop closure, which creates an unstable closed-loop system. Departure prevention procedures are quite different for the two cases; in the former case, positive control action is necessary for recovery, while a neutralization of control inputs might allow a recovery from the latter departure.

Figure 8 shows a departure caused by an aileron input. Normally, the result would be a significant negative roll rate,

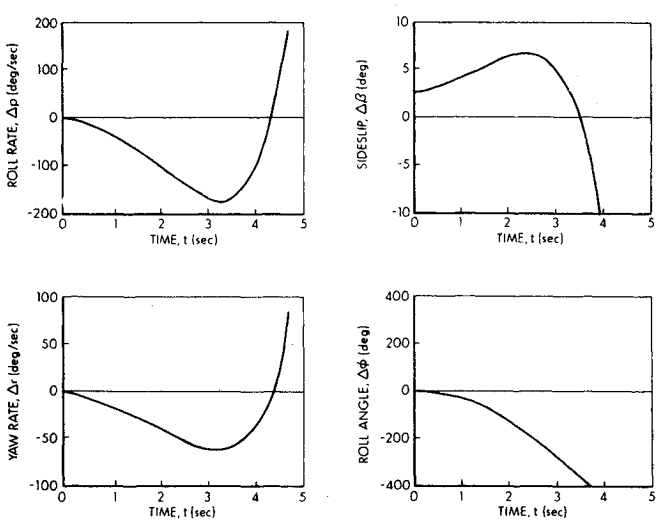

Fig. 6 An unforced departure due to directional instability.

but the sideslip and yaw rate build up so rapidly that the instability of the aircraft results in a rapid rolling departure with positive roll rate.

Prevention of Departure from Controlled Flight

There is ample reason to consider designing stability augmentation systems for the specific purpose of preventing departure. Aircraft design is dominated by performance requirements, and even unconstrained configuration modifications may not provide adequate stability or control response (especially during extreme maneuvering).

The powerful tools of linear-optimal control theory are applied to the problem in this section. The objective is to provide preliminary guidelines for DPSAS development, using the linear-optimal regulator. A linear-optimal regulator is a feedback control law of the form

$$\Delta u(t) = -K\Delta x(t) \tag{1}$$

where $\Delta u(t)$ is the vector of control command perturbations, $\Delta x(t)$ represents the vector of the aircraft's dynamic states, and K is the gain matrix, which scales the state measurements for proper stabilization and compensation of the aircraft's motion. This control law has several qualities that are desirable for the present study.[12] The control gains guarantee stability of the closed-loop system. Complete longitudinal/lateral-directional coupling is assumed and is accounted for in the design process. The control design technique identifies all significant crossfeeds and interconnects, as well as feedback gains. Tradeoffs between the amplitudes of state perturbations and of control motions are specified in the design process.

Linear-Optimal Regulator

A linear-optimal regulator can be designed for an aircraft near, at, or beyond its open-loop departure boundary. This design indicates the control loops that must be closed (either automatically or by the pilot) to prevent departure, providing asymptotic stability and minimizing a quadratic cost functional of the output and control. The DPSAS is not a limiter, because no limits are placed on the pilot's control authority, and it is not an automatic spin recovery system, because open-loop anti-spin control settings are not implemented. The DPSAS is intended to augment stability and to minimize the gyrations that precede loss of pilot control.

Design Equations

The basic design objective for the linear-optimal regulator is to define the feedback control law, which minimizes a quadratic cost functional J of the perturbation state vector $\Delta x(t)$ and the perturbation control vector $\Delta u(t)$:

$$J = \int_0^\infty [\Delta x^T(t) Q \Delta x(t) + \Delta u^T(t) R \Delta u(t)]\, dt \tag{2}$$

The control vector contains all available aircraft control displacements – in this case, throttle setting, elevator, aileron,

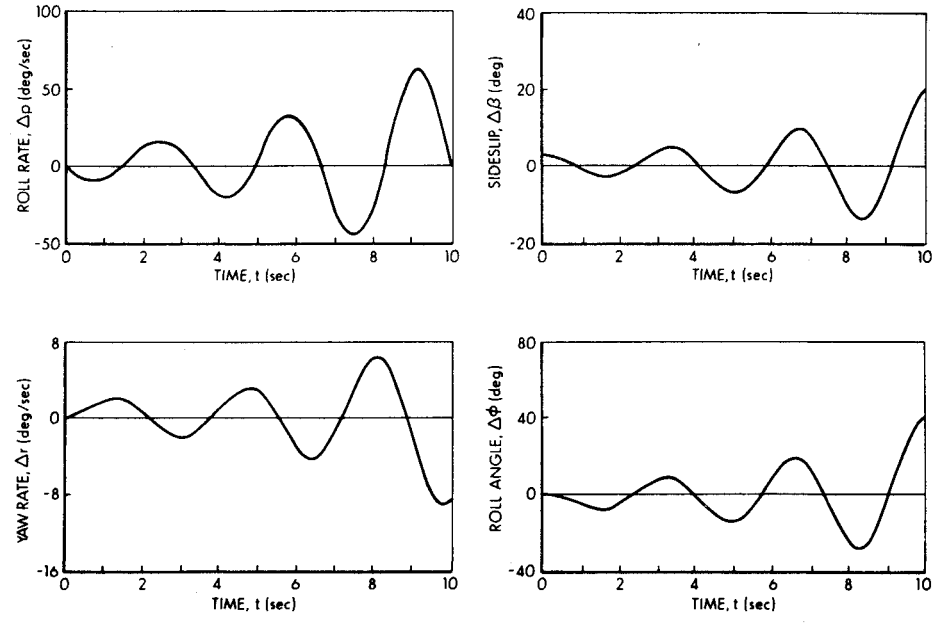

Fig. 7 An unforced departure due to negative Dutch roll damping.

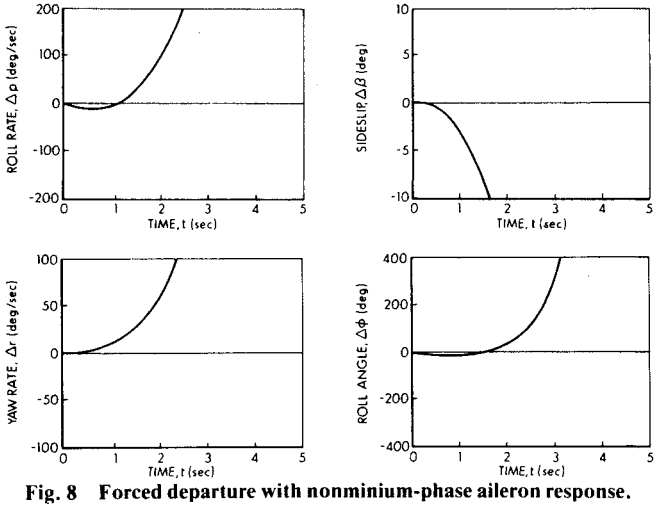

Fig. 8 Forced departure with nonminium-phase aileron response.

and rudder. The state vector is

$$\Delta x^T = [\Delta\theta \Delta u \Delta q \Delta w \Delta v \Delta r \Delta p \Delta\phi] \tag{3}$$

The state-weighting matrix Q is nonnegative-definitive and symmetric, and the control weighting matrix R is positive-definite and symmetric. Minimizing J minimizes the weighted sum of root-mean-square (rms) values of the state and control. This is loosely equivalent to a tradeoff between maximum allowable flight path perturbations and maximum control deflections.

The minimization of J must be accomplished subject to the dynamic constraint provided by the aircraft's linear equations of motion, expressed in state-space notation as

$$\Delta\dot{x}(t) = F\Delta x(t) + G\Delta u(t) \tag{4}$$

The gain matrix of the linear-optimal regulator is

$$K = R^{-1}G^T P \tag{5}$$

where the symmetric matrix P is the steady-state solution ($\dot{P} = 0$) of the matrix Riccati equation

$$\dot{P} = -PF - F^T P + PGR^{-1}G^T P - Q \tag{6}$$

The Kalman-Englar method has been used to solve Eq. (6).[12] The resulting DPSAS stabilizes the aircraft without using more control authority than that specified by R for state perturbations defined by Q.

The Q and R elements are used as design parameters that can be interpreted as the following maximum allowable perturbations: throttle setting, 100% of full scale; elevator deflection, 20°; aileron deflection, 60°; rudder deflection, 30°; Euler angle, 30°; body angular rate, 25 deg/sec; and body velocity, 9 m/sec. Table 2 indicates that the primary effects of the loop closures at the central flight conditions are to increase short period, Dutch roll, and phugoid damping and to quicken the roll and spiral modes.

The DPSAS gain matrix for this flight condition is listed in Table 3. The gain matrix illustrates why damping is increased in the closed-loop system: rate feedbacks are large. The classical longitudinal/lateral-directional partition can be observed in the gains. The elevator is seen to be the primary longitudinal controller, as throttle feedback gains are small (the principal effect of throttle control is to damp the phugoid mode). Lateral-directional control largely partitions along the roll and yaw axes. Although the gains shown in Table 3 have reasonable magnitudes, they could be reduced by reducing the values of q_{ii}. Transient response would be altered, but the system would remain stable.

Figure 9 shows that the lightly damped natural motion resulting from a 1° $\Delta\beta$ initial condition creates a substantial amount of roll as well as yaw. The regulator damps the oscillation and limits the roll angle excursion to 20% of its open-loop value, providing significant decoupling of lateral and directional motions.

DPSAS Control Laws

The control gains obtained at the central flight condition would stabilize the aircraft for some range of nominal angles and angular rates; however, changes in the aircraft's dynamics (reflected by variations in F and G) would lead to less-than-optimal regulation. It is necessary, therefore, to redesign the control gain matrix at each maneuvering condition in order to assess the full possibilities for preventing departure with the linear-optimal control law.

The separate maneuvering condition sweeps have been conducted using the reference aircraft flying at 6096 m and 94 m/sec in both cases. The first is a longitudinal sweep, in which a range of angles of attack and pitch rates is considered. The lateral-directional sweep varies sideslip angle and stability-

Table 2 Effects of DPSAS at the central flight condition[a]

Dynamic Mode	Open-Loop Characteristics			Closed-Loop Characteristics		
	Natural Frequency, rad/sec	Damping Ratio —	Time Constant, sec	Natural Frequency, rad/sec	Damping Ratio, —	Time Constant, sec
Short Period	1.17	0.35	—	2.67	0.72	—
Dutch Roll	2.25	0.03	—	2.35	0.60	—
Roll	—	—	2.26	—	—	0.36
Spiral	—	—	18.34	—	—	1.07
Phugoid	0.14	0.12	—	0.16	0.99	—

[a] $\alpha_0 = 15°$, $V_0 = 98$ m/sec, $h_0 = 6096$ m.

Table 3 DPSAS gain matrix at the central flight condition

Control Output	Pitch Angle, deg	Body x-Axis Velocity, m/s	Pitch Rate, deg/sec	Body z-Axis Velocity, m/s	Body y-Axis Velocity, m/s	Yaw Rate, deg/sec	Roll Rate, deg/sec	Roll Angle, deg
Throttle Setting, Fraction of Full Scale	-0.02	0.07	-0.01	0.02	0	0	0	0
Elevator Angle deg	-0.70	1.32	-1.54	-0.99	0	0	0	0
Aileron Angle, deg	0	0	0	0	-0.51	0.14	2.54	1.89
Rudder Angle, deg	0	0	0	0	1.94	-3.10	0.23	-0.10

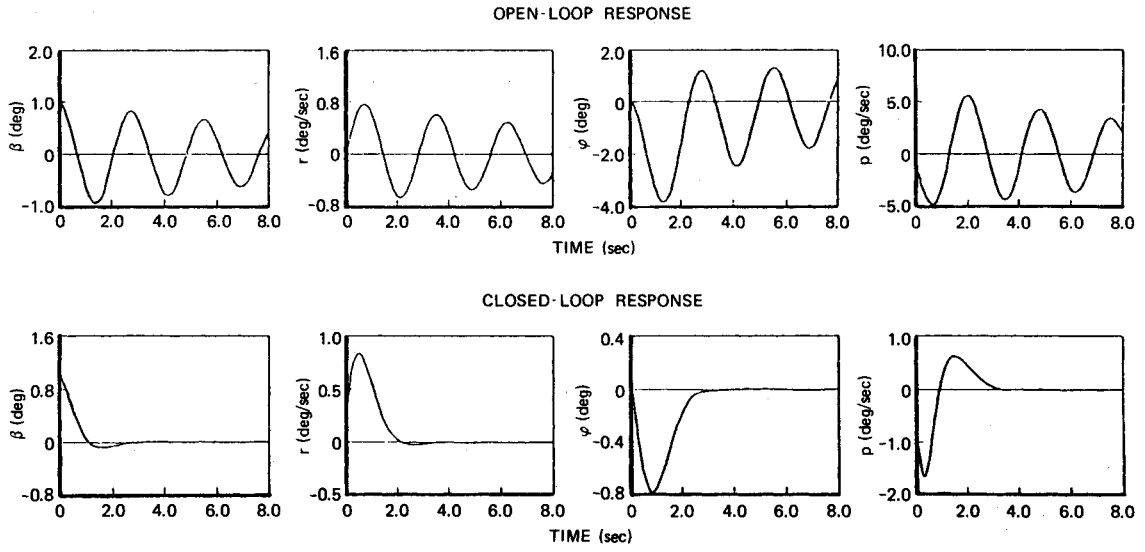

Fig. 9 Directional response at the central flight condition.

axis roll rate, introducing full coupling about all three axes. In the first sweep, control gains and closed-loop characteristics change, but the DPSAS structure is conventional, i.e., gains are partitioned along usual lines. The second sweep generates unconventional DPSAS structures as well as gain variations, since there is cross-axis coupling in the control paths.

Longitudinal Sweep

Closed-loop stability at 9 conditions is summarized by Table 4, where it can be seen that all modes are stable and at least moderately damped. Control power does not change with q_0, but it does change with α_0; consequently, the closed-loop stability at a given α_0 is relatively independent of q_0. There is a gradual decrease in Dutch roll damping as α_0 increases, and roll response becomes more sluggish. The roll and spiral modes combine to form a heavily damped complex pair at $\alpha_0 = 25°$. Spiral mode time constant is about 1 sec (stable) at $\alpha_0 = 5°$ and 15°; the phugoid mode also is stable.

The performance of the DPSAS in the pullup flight condition is assessed by comparing open- and closed-loop time responses. Figure 10 illustrates the aircraft's open- and closed-loop responses to an initial sideslip perturbation when α_0 is 15° and q_0 is 12 deg/sec. The oscillation grows at a moderate rate without stability augmentation but is damped in one cycle with the control loops closed.

Lateral-Directional Sweep

Table 5 presents the natural frequencies, damping ratios, and time constants of the aircraft with the linear-optimal regulator loops closed. The most striking result, in com-

Table 4 Closed-loop stability in the longitudinal sweep

Maneuver Condition		Short Period		Dutch Roll		Roll
α_o, deg	q_o, deg/sec	ω_n, rad/sec	ζ, —	ω_n, rad/sec	ζ, —	τ, sec
5	0	2.43	0.71	1.90	0.52	0.14
	12	2.43	0.69	1.95	0.53	0.14
	24	2.44	0.67	2.02	0.55	0.14
15	0	2.67	0.72	2.35	0.69	0.36
	12	2.67	0.71	2.42	0.67	0.37
	24	2.68	0.70	2.51	0.66	0.34
25	0	2.75	0.62	2.22	0.40	—
	12	2.78	0.61	2.23	0.39	—
	24	2.81	0.60	2.25	0.39	—

Table 5 Closed-loop stability in the lateral-directional sweep

Maneuver Condition		Short Period		Dutch Roll		Roll
β_o, deg	p_{w_o}, deg/sec	ω_n, rad/sec	ζ, —	ω_n, rad/sec	ζ, —	τ, sec
0	39	2.95	0.56	2.52	0.91	0.51
	26	2.79	0.60	2.35	0.84	0.40
	13	2.64	0.66	2.40	0.75	0.37
	0	2.67	0.72	2.35	0.69	0.36
10	-39	2.87	0.56	1.94	0.92	0.32
	-26	2.71	0.62	2.06	0.83	0.31
	-13	2.60	0.69	2.16	0.73	0.30
	0	2.63	0.73	2.16	0.67	0.30
	13	2.50	0.71	2.31	0.70	0.31
	26	2.65	0.61	2.25	0.81	0.32
	39	2.82	0.56	2.21	0.89	0.34

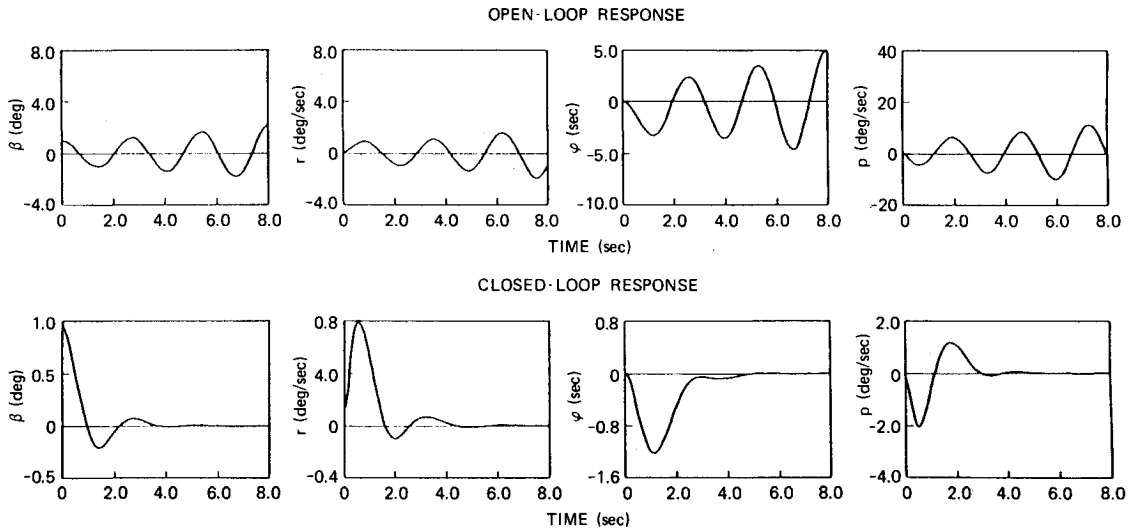

Fig. 10 Pitch-rate effect on directional response ($\alpha_0 = 15°$, $q_0 = 12$ deg/sec).

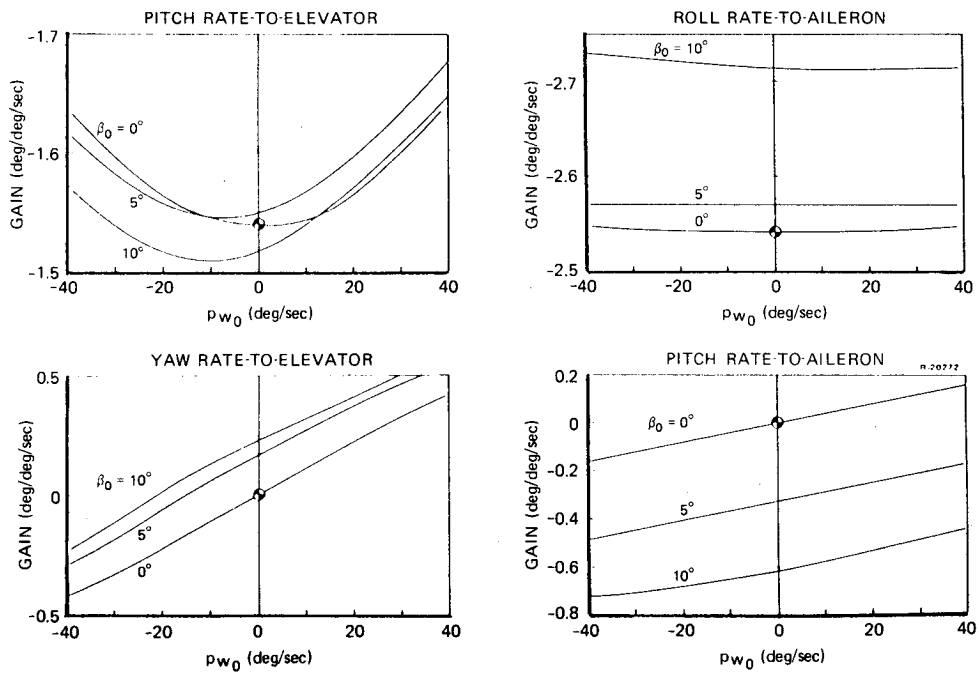

Fig. 11 Examples of gain variation in the lateral-directional sweep.

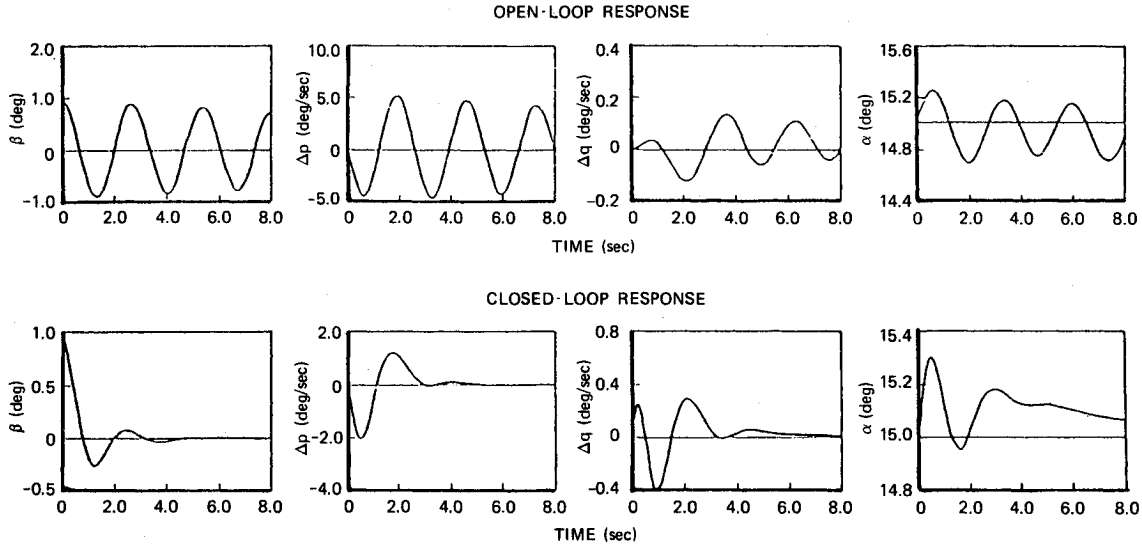

Fig. 12 Roll-rate effect on directional response ($\alpha_0 = 15°, \beta_0 = 0°, p_{w_0} = 39.6$ deg/sec).

parison with Table 4, is that the lateral-directional closed-loop roots evidence relatively little variation with maneuver condition. There are no roll-spiral or phugoid degeneracies, and all parameters stay within 40% of their mean values.

Examples of the DPSAS gain variations with sideslip angle and roll rate are plotted in Fig. 11. The most apparent trend is that primary gains, i.e., those which would be nonzero in symmetric flight, change very little with β_0 and p_{w_0}, whereas crossfeed gains have substantial variation with maneuver condition.

The crossfeed gains are shown to be nontrivial for even moderate values of β_0 and p_{w_0}, and those shown in Fig. 11 can be interpreted as nonlinear control elements. Note that each gain could be approximated by a function of the form

$$\text{gain} = c_1\beta_0 + c_2 p_{w_0} \tag{7}$$

where c_1 and c_2 are appropriate constants.

Figure 12 shows that roll rate introduces substantial longitudinal response to a directional input. The DPSAS damps the oscillation within 1½ cycles, although exitation of the phugoid mode leads to a slow decay in $\Delta\alpha$.

Conclusions

The key to linearizing the dynamics of the aircraft is that a quasisteady flight condition can be used as a reference path. The linear model provides a good description of the aircraft's perturbation response (to initial conditions, control inputs, and disturbances), even when the aircraft has large α, β, and angular rates; however, care must be exercised in computing a generalized trim condition to define the reference point.

An adaptive control design procedure, using the linear-optimal regulator for fixed-point design plus gain scheduling, is shown to provide a nonlinear control structure containing crossfeeds, as well as feedback gains. The resulting DPSAS has similarities to the flight control systems of current high-performance aircraft. However, the new design is based on "quadratic synthesis" techniques, which provide a unified set of control gains for all axes from a single set of vector-matrix design equations. The linear-optimal control law can be extended readily to a full command augmentation system, which provides satisfactory handling qualities, accounts for control actuator rate limits, and allows essentially unlimited pilot control authority (within the physical limitations of the aircraft). This and the mechanization of the control logic presented here are subjects for further study. The linear-optimal DPSAS prevents departure not by limiting the maneuvering ability of the aircraft, but by stabilizing the aircraft in all foreseeable maneuver conditions.

Acknowledgment

This work was conducted under Contract No. NAS1-13618 for the NASA Langley Research Center.

References

[1] Stengel, R. F. and Berry, P. W., "Stability and Control of Maneuvering High-Performance Aircraft," NASA CR-2788, April 1977.

[2] Phillips, W. H., "Effect of Steady Rolling on Longitudinal and Directional Stability," NACA TN 1627, June 1948.

[3] Abzug, M. J., "Effects of Certain Steady Motions on Small-Disturbance Airplane Dynamics," *Journal of the Aeronautical Sciences*, Vol. 21, Nov. 1954, pp. 749-762.

[4] Stengel, R. F., "Effect of Combined Roll Rate and Sideslip Angle on Aircraft Flight Stability," *Journal of Aircraft*, Vol. 12, Aug. 1975, pp. 683-685.

[5] Johnston, D. E. and Hogge, J. R., "Nonsymmetric Flight Influence on High Angle of Attack Handling and Departure," *Journal of Aircraft*, Vol. 13, Feb. 1976, pp. 112-118.

[6] Chambers, J. R. and Anglin, E. L., "Analysis of Lateral-Directional Stability Characteristics of a Twin-Jet Fighter Airplane at High Angles of Attack," NASA TN D-5361, Aug. 1969.

[7] Taylor, C. R. (ed.), "Aircraft Stalling and Buffeting," AGARD LS-74, Neuilly-sur-Seine, Feb. 1975.

[8] Gilbert, W. P. and Libbey, C. E., "Investigation of an Automatic Spin-Preventing System for Fighter Airplanes," NASA TN D-6670, March 1972.

[9] Lamars, J. P., "Design for Departure Prevention in the YF-16," AIAA Paper No. 74-794, Aug. 1974.

[10] DeRusso, P. M., Roy, R. J., and Close, C. M., *State Variables for Engineers*, John Wiley, New York, 1967.

[11] Eney, J. A. and Chambers, J. R., "Piloted Simulation of Spin," ASD Stall/Post-Stall/Spin Symposium, Wright-Patterson Air Force Base, Dec. 1971.

[12] Kwakernaak, H. and Sivan, R., *Linear Optimal Control Systems*, Wiley-Interscience, New York, 1972.